

05,13

## Nonreciprocal propagation of spin waves in a magnonic structure of two laterally coupled waveguides covered with a metal layer

© S.A. Odintsov, A.S. Ptashenko, A.V. Sadovnikov

Saratov National Research State University,  
Saratov, Russia

E-mail: odinoff@gmail.com

Received April 18, 2024

Revised April 18, 2024

Accepted May 8, 2024

The design of a unidirectional magnonic coupler in the form of YIG (yttrium iron garnet) waveguides with lateral coupling covered with a metal layer is proposed. The studied structure features unidirectional coupling that may be controlled by the external magnetic field direction, which was verified numerically and experimentally. The process of propagation of a spin-wave signal in it is associated with strong nonreciprocity, which manifests itself as changes in the amplitude-frequency response observed when the external magnetic field direction is varied. It is also demonstrated how the dynamic magnetization profile of a spin wave changes when the direction of propagation is reversed. The obtained results illustrate the feasibility of fabrication of nonreciprocal magnonic devices, such as multichannel magnonic couplers, multiplexers, and logic devices based on them, from a metallized structure.

**Keywords:** magnonics, planar systems, unidirectionality, magnetic field, multilayer systems.

DOI: 10.61011/PSS.2024.08.59041.55HH

### 1. Introduction

A spin wave (SW) is formed by magnetization oscillations propagating due to exchange and/or dipole interactions [1,2]. The results of studies of spin moment transfer in planar and multilayer magnetic structures suggest that the phenomena of interference and transient processes may be used to design magnonic networks utilizing the amplitude and phase of SWs as data carriers [3–6]. Owing to the tunability of spin-wave characteristics and the variation of wavelengths from micrometers to nanometers in the gigahertz frequency range, SWs have potential applications in data processing devices based on neuromorphic, reservoir, quantum, and wave concepts [7–9].

The propagation of magnetostatic surface waves (MSSWs), which are also known as Damon–Eshbach (DE) surface waves [10], is nonreciprocal due to exponential attenuation of the SW amplitude [11]. In the MSSW configuration, the direction of magnetization lies in the film plane and is perpendicular to the wave vector. The SW amplitude distribution over the film thickness has a maximum near the surfaces for waves with opposite directions of wave vector  $\mathbf{k}$  or magnetic field  $H_0$ , while frequencies  $f$  of oppositely directed waves are equal:  $f(\mathbf{k}) = f(-\mathbf{k})$ . It is known that the amplitude distribution over thickness for the DE mode is asymmetric relative to the central film plane, and the distribution of the electric field is also asymmetric. Therefore, if a metal layer is positioned near one of the surfaces of a ferromagnetic film, nonreciprocity may arise due to the difference in attenuation of oppositely directed SWs [12].

Nonreciprocity is an important property of magnetostatic spin waves, and their parameters depend significantly on the direction of propagation and the magnetic field. The ferromagnetic medium is gyrotropic and has a preferred direction determined by direction of the magnetic field. If one examines a unit magnetic moment precessing around the magnetic field and the projection of the magnetic moment onto a plane normal to the magnetic field moves counterclockwise, this precession should switch to clockwise direction when the magnetic field direction is reversed. Thus, when the direction of magnetic field changes, the dynamics of magnetization motion cannot be determined by simple symmetrical mapping. Spatial waveguide confinement is needed for the nonreciprocity effect to manifest itself in the propagation of spin waves. MSSWs are localized near one of the film surfaces; when the propagation direction changes, the MSSW field will be localized near the opposite surface. Although this does not affect the MSSW properties directly, the introduction of asymmetric boundary conditions (specifically, metallization of one of the surfaces) will reveal nonreciprocity. The amplitude nonreciprocity was noted in MSSWs excited by coplanar waveguides [12–14] and is attributable to the asymmetric efficiency of excited SW moving in opposite directions [15] and/or interference between the in-plane and out-of-plane components of dynamic magnetization.

The nonreciprocity of SWs propagating primarily in a certain direction set by the orientation of the magnetic field was demonstrated in structures with helical equilibrium magnetization [16,17], Dzyaloshinskii–Moriya interfacial in-

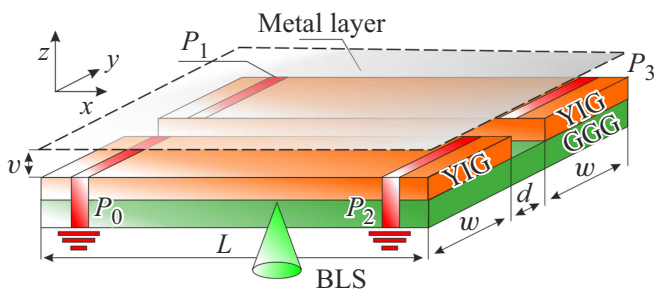


**Figure 1.** Schematic diagram of the examined structure.

teraction in ultrathin magnetic films [18], and magnonic crystals [12,19,20].

The specifics of propagation of spin waves in asymmetric magnonic structures and two-layer films with partial metallization were examined in [21,22]. The present study differs from those mentioned above in that it is focused on evaluating the feasibility of control over spin-wave transport in a lateral structure, which may act as a coupler of data signals. This implementation of nonreciprocal spin-wave transport may be used to design unidirectional magnonic coupling devices. In the present paper, we examine the nonreciprocal properties of SWs propagating in a laterally coupled system of waveguides covered with metal. It is demonstrated experimentally and numerically that unidirectional coupling, which is controlled easily by the external magnetic field direction, may be established in the proposed structure. Such systems may serve as building blocks for magnonic computing architectures utilizing nonreciprocal propagation of spin waves.

## 2. Structure under study

The schematic diagram of the studied structure is shown in Figure 1. Two parallel waveguides S1 and S2 made of yttrium iron garnet (YIG) (with a length of 8 mm, width  $w = 200\mu\text{m}$ , and thickness  $t = 10\mu\text{m}$ ) are positioned laterally parallel to each other with gap  $d_0$  on a gadolinium gallium garnet substrate (GGG). The metal layer is located above the lateral structure with air gap  $d$  between them. Microstrip antennas  $30\mu\text{m}$  in width (red regions on S1 in Figure 1) used for measurements were positioned in the input and output cross section of the S1 strip in such a way that only the S1 waveguide was excited. The attenuation parameter was  $\alpha = 10^{-5}$ , which corresponds to the measured value of the resonance line width (0.5 Oe) for YIG [1]. The distance between the input and output transducers was 5 mm. External magnetic field  $H_0 = 1200\text{ Oe}$  was applied along axis  $x$  of the waveguides.

## 3. Numerical modeling method

Numerical modeling was carried out by solving a system of Maxwell’s equations by the finite element method (FEM) in COMSOL Multiphysics. The dispersion characteristics were calculated with account for the fact that the frequency dependence of the electromagnetic field components follows the harmonic law [23]. The equation for the electric field vector has the following form:

$$\nabla \times (\hat{\mu} \nabla \times \mathbf{E}) - k^2 \epsilon \mathbf{E} = \mathbf{0},$$

where  $k = \omega/c$  is the wave number in vacuum,  $\omega = 2\pi/f$  is the angular frequency,  $f$  is the electromagnetic wave frequency, and  $\epsilon$  is the effective permittivity value. The

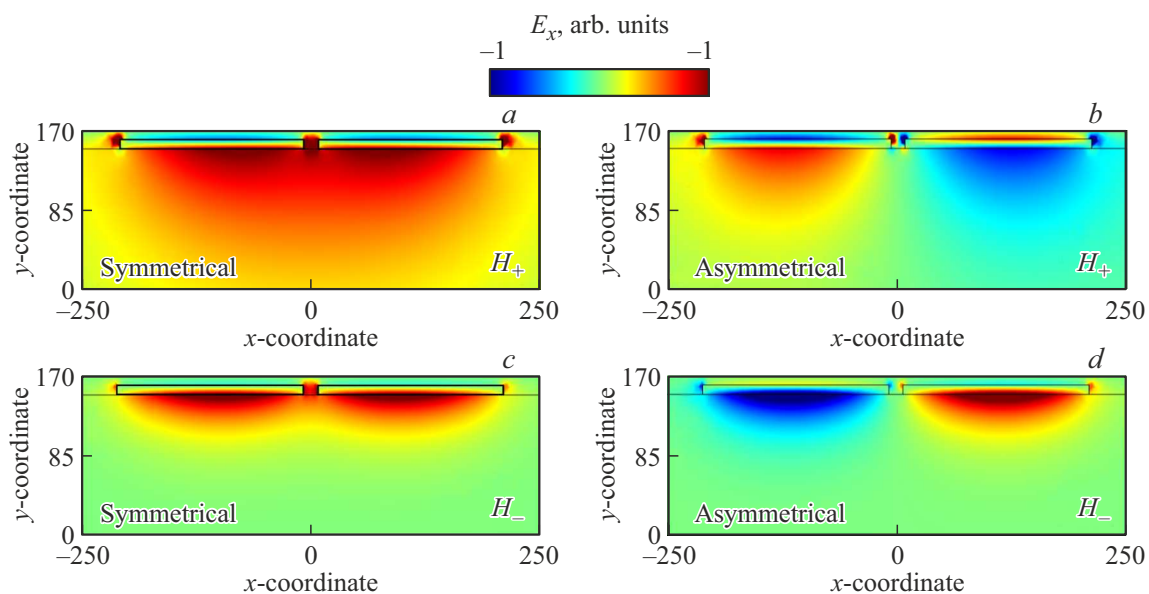


**Figure 2.** Distribution of component  $E_x$  of the electric field for symmetric and antisymmetric modes and opposite directions of the external magnetic field.

magnetic permeability tensor for tangential magnetization then takes the form

$$\hat{\mu} = \begin{vmatrix} \mu(f) & -i\mu_1(f) & 0 \\ i\mu_1(f) & \mu(f) & 0 \\ 0 & 0 & 1 \end{vmatrix},$$

$$\mu(f) = \frac{-f_B(f_B + f_M) - f^2}{f_B^2 - f^2}, \quad \mu_1(f) = \frac{f_M f}{f_B^2 - f^2},$$

$$f_M = \gamma 4\pi M_0, \quad f_B = \gamma H_{\text{int}}(x),$$

where  $\gamma$  is the gyromagnetic ratio,  $M_0$  is the saturation magnetization, and  $H_{\text{int}}$  is the internal magnetic field.

It should be noted that this method allows one to perform calculations with account for an inhomogeneous distribution of the internal magnetic field.

The finite element method for calculation of the eigen-wave spectrum in magnetic microwaveguides is suitable for analyzing eigenwaves and power transmission processes in the frequency domain near the beginning of the spin-wave spectrum (i. e., at  $k \approx k_0\sqrt{\varepsilon}$ ) and is most efficient in the case of film magnetic waveguides with layer thicknesses on the order of several micrometers or tens of micrometers [24].

#### 4. Experimental study

A microstrip antenna with a width of  $30 \mu\text{m}$  was installed in the input section of the studied structure to examine the effect of the field direction on the properties of spin waves. A microwave signal was fed to this antenna. The structure was magnetized tangentially by an external magnetic field produced by a GMW 3472-70 electromagnet. The field was directed along the  $x$  axis to excite MSSWs. An output antenna was used for signal reception in microwave experiments.

#### 5. Results

Figure 2 shows the distributions of the  $E_x$  electric field component for symmetric and antisymmetric modes of the dispersion characteristics of spin waves propagating in the structure under study. These distributions were obtained using the finite element method. The results for positive and negative directions of the external magnetic field at the same frequency are presented. It can be seen that the mode distributions corresponding to different directions of the field differ greatly, which is indicative of pronounced nonreciprocity in wave propagation.

Figure 3 shows the frequency dependence of the coefficient of transmission of SWs through waveguide S1 measured using a vector network analyzer with  $H_0$  applied in the negative direction of axis  $y$  and in the positive direction of axis  $y$ . The presented response of coupled waveguides is typical of a whole class of devices with linear and nonlinear coupling between modes. A well-pronounced

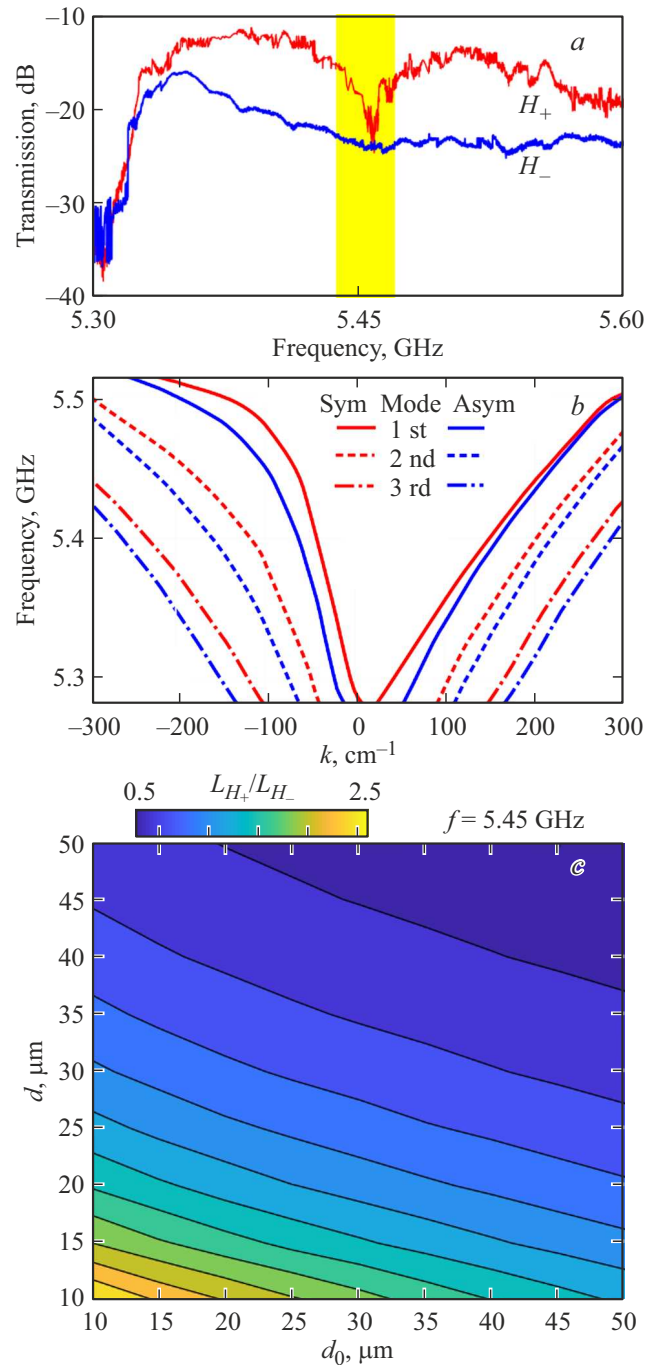


**Figure 3.** *a* — Coefficient of transmission of SWs through waveguide S1 measured experimentally for propagation in the negative direction of axis  $x$  (solid blue curve) and the positive direction of axis  $x$  (solid red curve); *b* — dispersion characteristics of the first three modes of spin waves in the positive and negative directions of SW propagation obtained via FEM modeling; *c* — map of the  $L_{H_+}/L_{H_-}$  coupling length coefficient with various geometric parameters at frequency  $f = 5.45 \text{ GHz}$ .

dip corresponds to frequencies at which the SW power does not reach the output section of waveguide S1.

It should be noted that the spectrum of eigenmodes of two identical waveguides consists of symmetric and

antisymmetric transverse modes. The symmetric mode in the  $x$  direction corresponds to the case when the amplitudes of magnetic potentials in two YIG films have the same phase (along the  $x$  axis); in the antisymmetric mode, they differ in phase by  $180^\circ$ .

Figure 3, *b* presents the results of numerical modeling of the studied structure in the form of dispersion characteristics of the first three SW modes in the positive and negative directions of SW propagation along axis  $x$ . The effect of nonreciprocity is seen clearly in this figure. Specifically, the wavenumbers of opposite waves differ by a factor of almost 3 at a frequency of 5.4 GHz, which indicative of a pronounced nonreciprocal nature of SW propagation in the studied structure. The parameter characterizing the propagation of waves with energy transfer from one waveguide to another is called the coupling length, which is equal in value to the distance at which the SW energy is transferred completely from one strip to another. It may be expressed as  $L = \frac{\pi}{k_s - k_{as}}$ , where  $k_s$  is the wavenumber of the symmetric mode and  $k_{as}$  is the wavenumber of the asymmetric mode.

It is also important to assess the influence of geometric gaps in the system on the coupling length. The results of examination of these dependences are presented in Figure 3, *c* in the form of maps of the  $L_+/L_-$  coupling length coefficient ( $L_+$  is the coupling length with the field directed along positive axis  $y$  and  $L_-$  is the coupling length with the field directed along negative axis  $y$ ) at different gap widths ( $d, d_0$ ) and a frequency of 5.4 GHz. These results illustrate the importance of choosing the proper geometric parameters to control the nonreciprocity effect in the most efficient way.

## 6. Conclusion

The results of experimental and numerical calculations revealed that the efficiency of nonreciprocal propagation of SWs in a coupled structure with a metal layer above it may be increased by altering the magnetic field direction. The effect of nonreciprocal SW propagation at the interface with the overlying metallic layer is thus established. It is possible to implement a simple method for controlling the nonreciprocal propagation of spin waves via geometry and equilibrium configuration in such a system. The obtained results verified the feasibility of construction of devices that utilize the properties of nonreciprocity. These devices may serve as multichannel magnonic couplers, multiplexers, and logic devices based on them. An in-depth study of this type of systems is needed to optimize their design and tailor it to the required dimensions and functionality that are necessary in specific applications in signal processing systems.

## Funding

This study was supported financially by grant No. 23-29-00610 from the Russian Science Foundation.

## Conflict of interest

The authors declare that they have no conflict of interest.

## References

- [1] A.G. Gurevich, G.A. Melkov. Magnetization Oscillations and Waves. CRC Press, London (1996).
- [2] D.D. Stancil, A. Prabhakar. Spin Waves: Theory and Applications. Springer Science & Business Media (2009).
- [3] A. Chumak, P. Kabos, M. Wu, C. Abert, C. Adelman, A.O. Adeyeye, J. Åkerman, F.G. Aliev, A. Anane, A. Awad, C.H. Back, A. Barman, G.E.W. Bauer, M. Becherer, E.N. Beginin, V.A.S.V. Bittencourt, Y.M. Blanter, P. Bortolotti, I. Boventer, D.A. Bozhko, S.A. Bunyayev, J.J. Carmiggelt, R.R. Cheenikundil, F. Ciubotaru, S. Cotozana, G. Csaba, O.V. Dobrovolskiy, C. Dubs, M. Elyasi, K.G. Fripp, H. Fulara, I.A. Golovchanskiy, C. Gonzalez-Ballester, P. Graczyk, D. Grundler, P. Gruszecki, G. Gubbiotti, K. Guslienko, A. Haldar, S. Hamdioui, R. Hertel, B. Hillebrands, T. Hioki, A. Houshang, C.-M. Hu, H. Huebl, M. Huth, E. Iacocca, M.B. Jungfleisch, G.N. Kakazei, A. Khitun, R. Khymyn, T. Kikkawa, M. Kläui, O. Klein, J.W. Klos, S. Knauer, S. Koraltan, M. Kostylev, M. Krawczyk, I.N. Krivorotov, V.V. Kruglyak, D. Lachance-Quirion, S. Ladak, R. Lebrun, Y. Li, M. Lindner, R. Macêdo, S. Mayr, G.A. Melkov, S. Mieszczyk, Y. Nakamura, H.T. Nembach, A.A. Nikitin, S.A. Nikitov, V. Novosad, J.A. Otálora, Y. Otani, A. Papp, B. Pigeau, P. Pirro, W. Porod, F. Porrati, H. Qin, B. Rana, T. Reimann, F. Riente, O. Romero-Isart, A. Ross, A.V. Sadovnikov, A.R. Safin, E. Saitoh, G. Schmidt, H. Schultheiss, K. Schultheiss, A.A. Serga, S. Sharma, J.M. Shaw, D. Suess, O. Surzhenko, K. Szulc, T. Taniguchi, M. Urbánek, K. Usami, A.B. Ustinov, T. van der Sar, S. van Dijken, V.I. Vasyuchka, R. Verba, S. Viola Kusminskiy, Q. Wang, M. Weides, M. Weiler, S. Wintz, S.P. Woloski, X. Zhang. Advances in Magnetism Roadmap on Spin-Wave Computing. IEEE Trans. Magn. **58**, 6, 0800172 (2022).
- [4] V.V. Kruglyak, S.O. Demokritov, D. Grundler. J. Phys. D **43**, 26, 264001 (2010).
- [5] A. Barman, G. Gubbiotti, S. Ladak, A.O. Adeyeye, M. Krawczyk, J. Gräfe, C. Adelman, S. Cotozana, A. Naeemi, V.I. Vasyuchka, B. Hillebrands, S.A. Nikitov, H. Yu, D. Grundler, A.V. Sadovnikov, A.A. Grachev, S.E. Sheshukova, J.-Y. Duquesne, M. Marangolo, G. Csaba, W. Porod, V.E. Demidov, S. Urazhdin, S.O. Demokritov, E. Al-bisetti, D. Petti, R. Bertacco, H. Schultheiss, V.V. Kruglyak, V.D. Poimanov, S. Sahoo, J. Sinha, H. Yang, M. Münzenberg, T. Moriyama, S. Mizukami, P. Landeros, R.A. Gallardo, G. Carlotti, J.-V. Kim, R.L. Stamps, R.E. Camley, B. Rana, Y. Otani, W. Yu, T. Yu, G.E.W. Bauer, C. Back, G.S. Uhrig, O.V. Dobrovolskiy, B. Budinska, H. Qin, S. van Dijken, A.V. Chumak, A. Khitun, D.E. Nikonov, I.A. Young, B.W. Zingsem, M. Winklhofer. J. Phys.: Condens. Matter **33**, 41, 3001 (2021).
- [6] K.O. Nikolaev, S.R. Lake, G. Schmidt, S.O. Demokritov, V.E. Demidov. Nano Lett. **23**, 8719 (2023).
- [7] S.A. Nikitov, A.R. Safin, D.V. Kalyabin, A.V. Sadovnikov, E.N. Beginin, M.V. Logunov, M.A. Morozova, S.A. Odintsov, S.A. Osokin, A.Yu. Sharaevskaya, Yu.P. Sharaevsky, A.I. Kirilyuk. Phys. — Usp. **63**, 10, 945 (2020).

- [8] B. Divinskiy, G. Chen, S. Urazhdin, S.O. Demokritov, V.E. Demidov. *Phys. Rev. Appl.* **14**, 4, 044016 (2020).
- [9] V.E. Demidov, S. Urazhdin, A. Anane, V. Cros, S.O. Demokritov. *J. Appl. Phys.* **127**, 17, 170901 (2020).
- [10] R.W. Damon, J.R. Eshbach. *J. Phys. Chem. Solids* **19**, 3–4, 308 (1961).
- [11] R. Camley. *Surf. Sci. Rep.* **7**, 3–4, 103 (1987).
- [12] M. Mruczkiewicz, P. Graczyk, P. Lupo, A. Adeyeye, G. Gubbiotti, M. Krawczyk. *Phys. Rev. B* **96**, 10, 104411 (2017).
- [13] M. Nakayama, K. Yamanoi, S. Kasai, S. Mitani, T. Manago. *Jpn. J. Appl. Phys.* **54**, 8, 083002 (2015).
- [14] K. Shibata, K. Kasahara, K. Nakayama, V.V. Kruglyak, M.M. Aziz, T. Manago, *J. Appl. Phys.* **124**, 24, 243901 (2018).
- [15] T. Schneider, A.A. Serga, T. Neumann, B. Hillebrands, M.P. Kostylev. *Phys. Rev. B* **77**, 21, 214411 (2008).
- [16] M.M. Salazar-Cardona, L. Körber, H. Schultheiss, K. Lenz, A. Thomas, K. Nielsch, A. Kákay, J.A. Otálora. *Appl. Phys. Lett.* **118**, 26, 262411 (2021).
- [17] N. Ogawa, L. Köhler, M. Garst, S. Toyoda, S. Seki, Y. Tokura. *Proceed. National Acad. Sci.* **118**, 8, e2022927118 (2021).
- [18] M. Kuepferling, A. Casiraghi, G. Soares, G. Durin, F. Garcia-Sanchez, L. Chen, C.H. Back, C.H. Marrows, S. Tacchi, G. Carlotti. *Rev. Mod. Phys.* **95**, 1, 015003 (2023).
- [19] M. Mruczkiewicz, M. Krawczyk, G. Gubbiotti, S. Tacchi, Y.A. Filimonov, D.V. Kalyabin, I.V. Lisenkov, S.A. Nikitov. *New J. Phys.* **15**, 11, 113023 (2013).
- [20] I. Lisenkov, D. Kalyabin, S. Osokin, J. Klos, M. Krawczyk, S. Nikitov. *J. Magn. Magn. Mater.* **378**, 313 (2015).
- [21] A.A. Grachev, A.V. Sadovnikov. *Phys. Solid State* **65**, 1849 (2023).
- [22] A.S. Ptashenko, S.A. Odintsov, E.H. Lock, A.V. Sadovnikov. *Phys. Solid State* **66**, 1, 76 (2024).
- [23] A.V. Sadovnikov, K.V. Bublikov, E.N. Beginin, S.A. Nikitov. *J. Commun. Technol. Electron.* **59**, 9, 914 (2014).
- [24] A.V. Sadovnikov, E.N. Beginin, M.A. Morozova, Yu.P. Sharaevskii, S.V. Grishin, S.E. Sheshukova, S.A. Nikitov. *Appl. Phys. Lett.* **109**, 4, 042407 (2016).

*Translated by D.Safin*